

Optical Monte Carlo modeling of a true port wine stain anatomy

Jennifer Kehlet Barton, T. Joshua Pfefer, Ashley J. Welch

*Biomedical Engineering Program, The University of Texas at Austin, Austin, TX 78712
jbarton@mail.utexas.edu*

Derek J. Smithies, J. Stuart Nelson

Beckman Laser Institute and Medical Clinic, University of California, Irvine, CA 92612

Martin J.C. van Gemert

Academic Medical Center, University of Amsterdam, Amsterdam, The Netherlands

Abstract: A unique Monte Carlo program capable of accommodating an arbitrarily complex geometry was used to determine the energy deposition in a true port wine stain anatomy. Serial histologic sections taken from a biopsy of a dark red, laser therapy resistant stain were digitized and used to create the program input for simulation at wavelengths of 532 and 585 nm. At both wavelengths, the greatest energy deposition occurred in the superficial blood vessels, and subsequently decreased with depth as the laser beam was attenuated. However, more energy was deposited in the epidermis and superficial blood vessels at 532 nm than at 585 nm.

©1998 Optical Society of America

OCIS code: (170.3660) Light propagation in tissues; (170.1870) Dermatology; (170.1610) Clinical applications

References and links

1. M.J.C. van Gemert, A.J. Welch, O.T. Tan, J.A. Parrish, "Limitations of carbon dioxide lasers for treatment of port-wine stains," *Arch. Dermatol.* **123**, 71-73 (1987).
2. O.T. Tan, P. Morrison, A.K. Kurban "585 nm for the treatment of port-wine stains," *Plastic and Reconstructive Surg.* **86**, 1112-1117 (1990).
3. J.M. Garden, O.T. Tan, R. Kerschmann, J. Boll, H. Furumoto, R.R. Anderson, J.A. Parrish. "Effect of dye laser pulse duration on selective cutaneous vascular injury." *J. Invest. Dermatol.* **87**, 653-657 (1986).
4. O.T. Tan, M. Motemedi, A.J. Welch, A.K. Kurban, "Spotsize effects on guinea pig skin following pulsed irradiation," *J. Invest. Dermatol.* **90**, 877-881 (1988).
5. M.J.C. van Gemert, A.J. Welch, A.P. Amin, "Is there an optimal laser treatment for port wine stains?," *Lasers Surg. Med.* **6**, 76-83 (1986).
6. A. Kienle, R. Hibst, "A new optimal wavelength for treatment of port wine stains?," *Phys. Med. Biol.* **40**, 1559-1576 (1995).
7. C.C. Dierickx, J.M. Casparian, V. Venugopalan, W.A. Farinelli, R.R. Anderson, "Thermal relaxation of port-wine stain vessels probed in vivo: the need for 1-10-millisecond laser pulse treatment," *J. Invest. Dermatol.* **105**, 709-714 (1995).
8. M. Keijzer, J.W. Pickering, M.J.C. van Gemert, "Laser beam diameter for port wine stain treatment," *Lasers Surg. Med.* **11**, 601-605 (1991).
9. T.J. Pfefer, J.K. Barton, E.K. Chan, M.G. Ducros, B.S. Sorg, T.E. Milner, J.S. Nelson, A.J. Welch, "A three-dimensional modular adaptable grid numerical model for light propagation during laser irradiation of skin tissue," *IEEE J. Sel. Top. Quantum. Electron.* **2**, 934-942 (1996).
10. S.L. Jacques, L. Wang, "Monte Carlo modeling of light transport in tissues," in *Optical-Thermal Response of laser-irradiated tissue*, A.J. Welch and M.J.C. van Gemert, ed. (Plenum Press, New York 1995).
11. D.J. Smithies, M.J.C. van Gemert, M.K. Hansen, T.E. Milner, J. S. Nelson, "Three-dimensional reconstruction of port wine stain vascular anatomy from serial histological sections," *Phys. Med. Biol.* **12**, 1013-17 (1997).

12. M.J.C. van Gemert, A.J. Welch, J.W. Pickering, O.T. Tan, "Laser treatment of port wine stains," in *Optical-Thermal Response of laser-irradiated tissue*, A.J. Welch and M.J.C. van Gemert, ed. (Plenum Press, New York 1995).
 13. G.W. Lucassen, W. Verkrusse, M. Keijzer, M.J.C. van Gemert. "Light distributions in a port wine stain model containing multiple cylindrical and curved blood vessels," *Lasers Surg. Med.* **19**, 345-357 (1996).
 14. R.M. Adrian, E.A. Tanghetti. "Long pulse 532-nm laser treatment of facial telangiectasia," *Dermatol. Surg.* **24**, 71-74 (1998).
-

1. Introduction

Laser irradiation is currently the only acceptable treatment for port wine stains (PWS), a vascular malformation of the skin characterized by overabundant and/or enlarged blood vessels. Experimental [1-4] and analytical [5-8] efforts have led to the adoption of lasers with wavelengths in the green - orange spectrum, pulse durations in the range of 0.1 to 10 milliseconds, and large (3-10 mm) spotsizes. Although the avoidance of scarring and discoloration has improved, many patients still have unacceptable or incomplete fading of their PWS.

Monte Carlo modeling has been used to understand laser-tissue interaction and to predict optimal treatment parameters. Previous modeling of laser interaction with PWS has generally involved a simplified skin geometry consisting of slabs of epidermis and dermis, and regular arrays of cylindrical blood vessels. Novel modeling is needed to aid understanding of clinical results which are not in agreement with existing laser-tissue interaction analyses.

We have developed a unique optical Monte Carlo program which can simulate light propagation in any user-defined three-dimensional tissue geometry, and used this program to determine the volumetric energy deposition (W) at wavelengths of 532 and 585 nm in a model PWS generated from serial histologic sections.

2. Materials and methods

2.1 Optical Monte Carlo program

The optical Monte Carlo program is based on one described previously. [9] A material property matrix stores information about the spatial arrangement of tissue constituents. Each voxel in this matrix contains an integer that identifies the type of tissue at this location (e.g. 1 = dermis, 2 = blood, etc.). Photons propagate through the space represented by this matrix according to standard variable stepsize and weighted photon Monte Carlo rules. [10] If the photon crosses a voxel boundary and the tissue type changes, refraction or reflection may occur. A photon which reaches the lateral extent of the represented space (boundaries perpendicular to the surface of the tissue) is reflected back. Photons which reach the depth extent (boundary parallel to the tissue surface) of the represented space continue to propagate through a "buffer region" assumed to have properties of dermis. If the photon travels beyond a depth at which it is unlikely to return to the tissue region of interest, it is terminated. This method results in an approximation of an infinitely wide incident beam. The absorbed photon weight is converted to W [J/cm^3] and accumulated in an energy deposition matrix, which has the same dimensions as the material property matrix.

The material property matrix can be generated from mathematical constructs or actual data, such as digitized optical coherence tomography, confocal microscopy, or histological images. In this study, data were extracted from 6 μm thick histology sections taken from biopsy of a dark red, laser therapy resistant PWS. [11] Sections were photographed and digitized with 2 μm pixel resolution. The epidermis, dermis, and blood vessels were manually identified, and each pixel was assigned an integer value corresponding to its tissue type. Forty-two sections were combined to create a matrix representing a 0.25 mm X 0.25 mm X 0.5 mm deep volume of tissue. Figure 1 shows a three-dimensional representation of the material properties matrix. This skin representation differs from previously studied,

simplified geometry Monte Carlo models in that it has an irregular epidermis and complex blood vessel structure.

2.2 Simulation parameters

Two wavelengths currently used in PWS treatment were considered: 532 and 585 nm. An infinite, uniform beam profile with a radiant exposure of 1 J/cm^2 was chosen. Because the volume of tissue studied is small, the results obtained with an infinite beam are approximately the same as those determined with a 3 or 5 mm spot size, assuming that the tissue is located towards the center of the beam. The calculated values of W can be linearly scaled to any beam energy. Optical properties (absorption coefficient μ_a , scattering coefficient μ_s , anisotropy g , and index of refraction n) were chosen from the literature and are summarized in Table 1. [12,13]

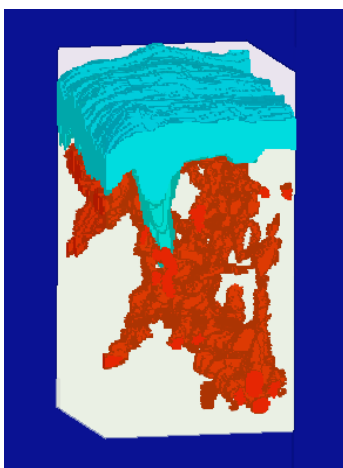


Fig. 1. A three dimensional rendering of the PWS material properties matrix is shown with epidermis and blood vessels in shades of blue and red, respectively. Air and dermis have been made transparent for clarity.

Table 1. Optical Properties

	μ_a (1/cm)	μ_s (1/cm)	g	n
Epidermis				
532 nm	21	530	0.77	1.37
585 nm	18	470	0.79	1.37
Dermis				
532 nm	2.2	156	0.77	1.37
585 nm	2.4	129	0.79	1.37
Blood				
532 nm	266	473	0.995	1.33
585 nm	191	467	0.995	1.33

3. Results

Figures 2 and 3 show Quicktime movies of the PWS anatomy energy deposition matrix at 532 nm and 585 nm, respectively. Regions of low energy deposition (W) have been made transparent for clarity. The movies show a rotating, three dimensional view of the entire matrix. Figures 4 and 5 are corresponding slices from centers of the 532 and 585 nm energy

deposition matrices, respectively. Figure 6 shows the W values for a single column taken from slices in Figures 4 and 5.

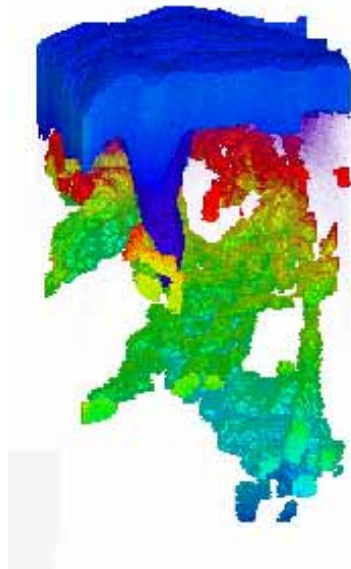


Fig. 2. Quicktime movie, energy deposition (J/cm^3) in a PWS with an infinite incident beam at 532 nm and $1 J/cm^2$ radiant exposure.

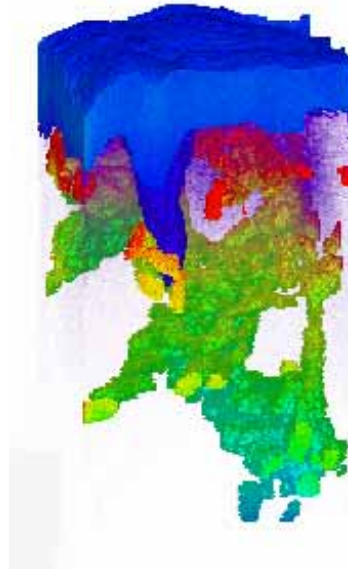


Fig. 3. Quicktime movie, energy deposition (J/cm^3) in a PWS with an infinite incident beam at 585 nm and $1 J/cm^2$ radiant exposure.

4. Discussion

At both wavelengths, some general trends can be noted. Energy deposition (W) decreases through the epidermis and dermis as the laser beam is attenuated. W is greater in the epidermis than the dermis, and highest in the superficial blood vessels. Decreased W in the dermis is due to the lower absorption coefficient and, to a lesser extent, attenuation in the laser beam as it passes through the epidermis. The large absorption coefficient of blood causes the highest W in the blood vessels at shallow (< 0.3 mm) depths despite attenuation in the epidermis and dermis.

In the smallest (10-20 μm) blood vessels, W appears reasonably constant. This can be explained by the penetration depth ($1/[\mu_a + \mu_s(1-g)]$) of laser light in blood, which for both wavelengths is about 45 μm . Thus, insufficient attenuation occurs for the effect to be noticeable. In the larger blood vessels, the decrease of W with depth becomes apparent. Also, at a constant depth, W can be greater at the vessel periphery than in the center. The scattering of the incident laser beam in the dermis causes light to enter the vessel from all angles. An interesting feature of this PWS anatomy is the clusters of small blood vessels. Because of competition for light, blood vessels in the center of clusters have reduced W compared to solitary vessels.

A comparison of the results for 532 nm and 585 nm reveals some differences due to the wavelength-dependent optical properties of tissue. At 532 nm, W in the epidermis is greater than at 585 nm. Since temperature rise and damage are related to energy deposition, there may be a greater risk of scarring with 532 nm. Epidermal cooling devices could be used to alleviate adverse effects. The reflectance at 532 nm (16.9 %) is also greater than 585 nm (16.0 %), owing in part to increased epidermal scattering. At 532 nm, blood vessel W is greater at shallow depths, but less at greater depths, than 585 nm. The larger absorption and

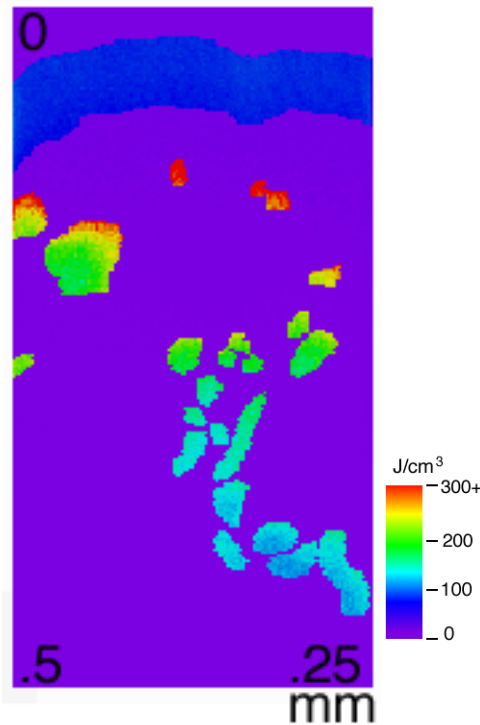


Fig. 4. A single transverse slice 0.25 mm wide by 0.5 mm deep of the energy deposition (J/cm^3) in a PWS. An infinite incident beam at 532 nm with $1 J/cm^2$ radiant exposure was simulated.

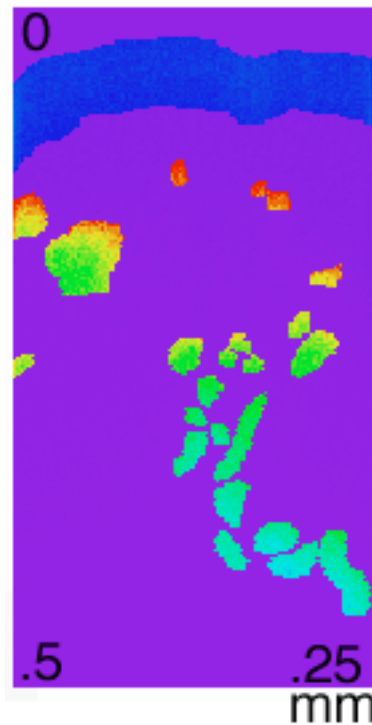


Fig. 5. A single transverse slice 0.25 mm wide by 0.5 mm deep of the energy deposition (J/cm^3) in a PWS. An infinite incident beam at 585 nm with $1 J/cm^2$ radiant exposure was simulated.

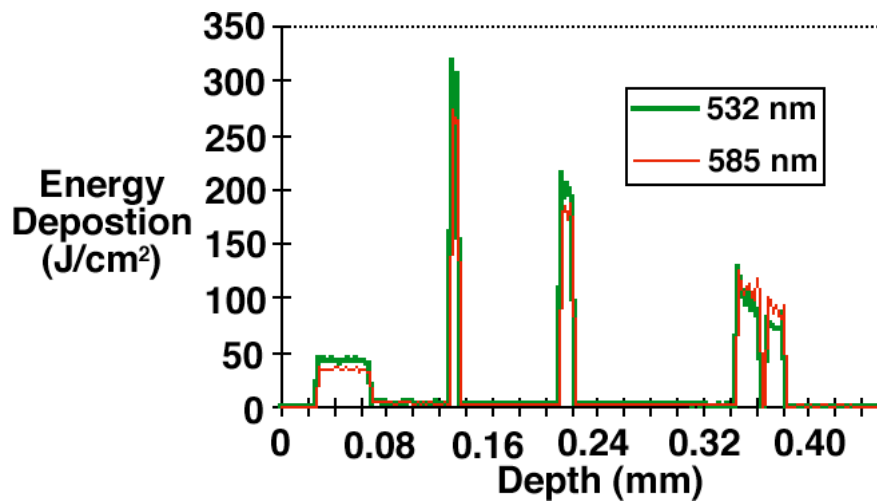


Fig. 6. Energy deposition (J/cm^3) for corresponding columns of the transverse slices shown in Figures 4 and 5. Infinite incident beam at 532 and 585 nm, with $1 J/cm^2$ radiant exposure.

scattering coefficients of 532 nm light in blood causes increased W at shallow depths. Deeper into the tissue, however, less light is available to the blood vessels. Lasers at both

wavelengths (but differing pulse durations, spot sizes, and energies) have been successfully used to treat vascular disorders. [2,14] A complete evaluation of the laser-tissue interaction requires a model which can incorporate laser pulse duration and thermal boundary conditions, including cooling.

5. Conclusion

The novel optical Monte Carlo program used in this study permits the simulation of photon propagation and energy deposition in arbitrarily complex geometries. A trade-off is made, however, with increased complexity of the tissues studied. The results presented above may present an extremely realistic determination of the energy deposition in this particular PWS, but complexity makes the results more difficult to interpret. Simulation results are also dependent upon the chosen optical property values, a range of which are found in the literature. We are currently developing a thermal model which will complement this optical Monte Carlo model by determining the tissue temperature history and thermal damage accumulation. Together with a non-invasive measurement technique such as optical coherence tomography, these programs may be used to estimate optimal laser parameters for the coagulation of a specific set of *in vivo* blood vessels.

Acknowledgments

Funding for this research was provided in part by grants from the Office of Naval Research Free Electron Laser Biomedical Science Program (N00014-91-J-1564), Department of Energy Center of Excellence for Medical Laser Applications (DE-FG03-95ER 61971), National Institutes of Health (R29-AR41638, R01-AR42437, R01-AR43419) and the Albert and Clemmie Caster Foundation.